

You might find this additional information useful...

This article cites 11 articles, 4 of which you can access free at:

<http://jap.physiology.org/cgi/content/full/91/6/2531#BIBL>

This article has been cited by 4 other HighWire hosted articles:

Wave intensity analysis of left ventricular filling: application of windkessel theory

J. A. Flewitt, T. N. Hobson, J. Wang Jr., C. R. Johnston, N. G. Shrive, I. Belenkie, K. H. Parker and J. V. Tyberg

Am J Physiol Heart Circ Physiol, June 1, 2007; 292 (6): H2817-H2823.

[Abstract] [Full Text] [PDF]

Assessment of left ventricular diastolic suction in dogs using wave-intensity analysis

Z. Wang, F. Jalali, Y.-H. Sun, J.-J. Wang, K. H. Parker and J. V. Tyberg

Am J Physiol Heart Circ Physiol, April 1, 2005; 288 (4): H1641-H1651.

[Abstract] [Full Text] [PDF]

Chasing the wave. Unfashionable but important new concepts in arterial wave travel

R. A. Bleasdale, K. H. Parker and C. J. H. Jones

Am J Physiol Heart Circ Physiol, June 1, 2003; 284 (6): H1879-H1885.

[Full Text] [PDF]

Pericardium modulates left and right ventricular stroke volumes to compensate for sudden changes in atrial volume

C. A. G. Kroeker, N. G. Shrive, I. Belenkie and J. V. Tyberg

Am J Physiol Heart Circ Physiol, June 1, 2003; 284 (6): H2247-H2254.

[Abstract] [Full Text] [PDF]

Medline items on this article's topics can be found at <http://highwire.stanford.edu/lists/artbytopic.dtl> on the following topics:

Physiology .. Blood Pressure

Medicine .. Anesthesia

Physics .. Ultrasonics

Updated information and services including high-resolution figures, can be found at:

<http://jap.physiology.org/cgi/content/full/91/6/2531>

Additional material and information about *Journal of Applied Physiology* can be found at:

<http://www.the-aps.org/publications/jappl>

This information is current as of January 5, 2008 .

Left ventricular wave speed

JUN-JR WANG,¹ KIM H. PARKER,² AND JOHN V. TYBERG¹

¹Department of Medicine and Physiology and Biophysics, University of Calgary, Calgary, Alberta, Canada T2N 4N1; and ²Physiological Flow Studies Group, Department of Bioengineering, Imperial College of Science, Technology and Medicine, London, SW7 2BY United Kingdom

Received 25 June 2001; accepted in final form 14 August 2001

Wang, Jiun-Jr, Kim H. Parker, and John V. Tyberg.

Left ventricular wave speed. *J Appl Physiol* 91: 2531–2536, 2001.—Left ventricular (LV) wave speed (LVWS) was studied experimentally and confirmed in theory. Combining the definition of elastance (E) with the equations for the conservation of mass and momentum shows that LVWS is proportional to the square root of ELA, where *L* is long-axis length and *A* is the cross-sectional area, and the density of the blood. (We defined $ELA = \gamma$, where γ is compressibility.) We studied nine open chest, anesthetized dogs, three of which were studied during caval constriction when LV end-diastolic pressure was ≤ 0 mmHg. The hearts were paced at ~ 90 beats/min, and LV cross-sectional area was measured by using two pairs of ultrasonic crystals; E was calculated from the LV pressure-area loop. A pulse generator was connected to the LV apex, and LVWS was measured by using two pressure transducers: one near the apex and the other near the base. Their distance was measured roentgenographically and compared with the diameter of a reference ball. LVWS ranged from ~ 1 m/s during diastole to ~ 10 m/s during systole. The slope of the log *c* (where *c* is wave speed) vs. log γ was 0.546, which is in agreement with theory (0.5). When $\gamma \leq 0$, LVWS was ~ 1.5 m/s.

left ventricle; elastance; distensibility

BECAUSE THE LEFT VENTRICLE (LV) profoundly changes its elastance during the cycle of contraction and relaxation (13), wave speed must also change significantly. At present, there is only one report in the literature that relates wave speed to elastance, and those measurements were made during only a part of the cardiac cycle (10). As we intend to study LV diastolic filling and systolic ejection using wave-intensity analysis, we designed a protocol to measure wave speed during all phases of the cycle. Our findings are supported by a theoretical discussion.

METHODS

Instrumentation. The experiments were performed in nine healthy mongrel dogs weighing between 21 and 30 kg. Dogs were anesthetized by thiopental sodium (20 mg/kg) followed by fentanyl citrate ($30 \mu\text{g}\cdot\text{kg}^{-1}\cdot\text{h}^{-1}$) and ventilated with a 1:1 nitrous oxide-oxygen mixture with 1.6–2% of isoflurane. The rate of a constant-volume respirator (model 607, Har-

vard Apparatus, Natick, MA) (tidal volume, 15 ml/kg) was adjusted to maintain normal blood-gas tensions and pH. Body temperature was maintained at 37°C using a circulating-water warming blanket and a heating lamp. An albumin-saline solution was infused through the jugular vein to maintain the blood pressure.

A volume pulse generator was connected to the LV via a purse-string suture at the apex (Fig. 1). It consisted of a specially fabricated hollow cylinder with an inner diameter of 4.0 cm and volume of 153 ml, which contained a balloon that was connected to a counterpulsation pump (Datascope, Paramus, NJ). The cylinder was filled with blood, and all bubbles were carefully removed. Two catheter-tip manometers (SPC-482A, Millar Instruments, Houston, TX) were introduced retrogradely into the LV via the common carotid arteries, one near the apex and the other near the base (Fig. 1), and were referenced using their fluid-filled lumens so that absolute values of pressure could be ascertained. The tips of the two manometers were positioned on a straight line with the end of the nozzle, and the distance between them was measured on the radiograph. Two pairs of ultrasonic crystals (Sonometrics, London, Ontario) were implanted in the LV endocardium to measure the anterior-posterior and septum-free wall dimensions. The pericardium was then loosely sutured to approximate the normal constraint (9). The heart rate was controlled at ~ 90 beats/min by right atrial pacing. A two-channel laboratory stimulator (model S88, Grass Medical Instruments, Quincy, MA) was used to trigger the counterpulsation pump, which could be adjusted to inflate and deflate the balloon (duration, ~ 100 ms) at any chosen instant during the cardiac cycle. A smaller inflating volume was chosen during systole (5 ml) than during diastole (13 ml) to produce pressure increments of similar sizes. A pneumatic cuff (In Vivo Metric, Healdsburg, CA) was placed around the inferior vena cava (IVC).

At the end of experiment, the distance between the two manometer tips (assumed to be in the same horizontal plane) was measured from a single-plane, cut-film radiograph taken with the use of a fluoroscope and a metal ball of known diameter (1.90 cm) placed beside the LV as a reference. Knowing the time interval required for the wave to travel from one manometer to the other and the distance between them, we could calculate wave speed.

Experimental protocol. A series of IVC occlusions was performed to define LV elastance (see below). The dog was then allowed to recover for 3–5 min before we started the wave-speed measurements. The balloon could be inflated at any

Address for reprint requests and other correspondence: J. V. Tyberg, Professor of Medicine and Physiology and Biophysics, Univ. of Calgary Health Science Centre, 3330 Hospital Drive NW, Calgary, Alberta, Canada T2N 4N1 (E-mail: jtyberg@ucalgary.ca).

The costs of publication of this article were defrayed in part by the payment of page charges. The article must therefore be hereby marked “advertisement” in accordance with 18 U.S.C. Section 1734 solely to indicate this fact.

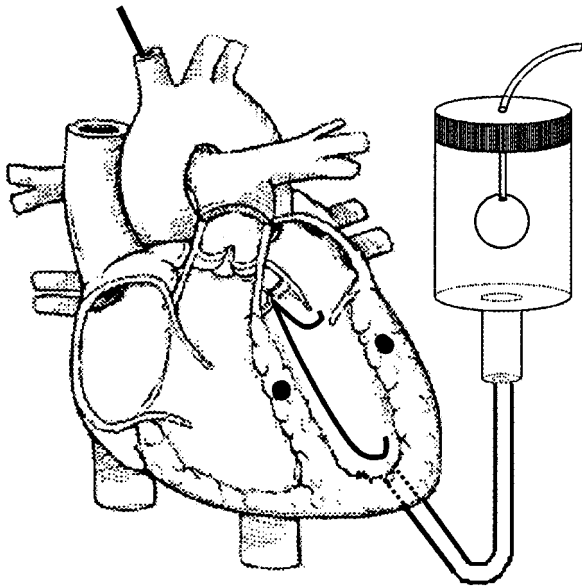


Fig. 1. Experimental setup. A pulse generator, which contains a balloon, was connected to the apex of the heart. A Lucite cylinder (inner diameter = 4 cm; volume = 153 ml) was connected to a thin steel tube (outer diameter = 1.27 cm), which was sutured into the left ventricular (LV) apex (dotted lines) and filled with blood. The balloon was connected to a counterpulsation pump. Two catheter-tip pressure transducers were introduced in the LV via common carotid arteries: one to the apex and the other to the base. These two transducers were positioned on a straight line with the nozzle of the pulse generator. Two pairs of crystals (solid dots, only one pair shown) were implanted to measure anterior-posterior and septum-to-free-wall diameter.

instant during the cardiac cycle, which we divided into 15 phases with respect to the marker on the pump. The experiment started by inflating the balloon at the beginning of systole. We then moved the inflation point to the next phase, fired the balloon, and then proceeded to the next phase until the whole cycle had been studied. Between each inflation, we allowed an interval of 3–5 min for recovery.

In three dogs, we reduced LV transmural diastolic pressures to negative values before measuring wave speed. Whereas profound arterial hypotension was avoided, the IVC was constricted until LV diastolic pressure became negative (–1 to –5 mmHg). This protocol was the same as that described above, except that measurements were made only during diastole.

In all experiments, we sought to achieve a quasi-steady state so that, later, we could subtract the pressure waveform of the previous control beat from that of the balloon inflation beat, thereby isolating the signal due to the generated pulse (see below).

Data analysis. After preamplification (model VR-16, Electronics to Medicine, Honeywell, White Plains, NJ), the analog hemodynamic signals were passed through an antialiasing, low-pass filter with a cutoff frequency of 500 Hz and were recorded using an Intel Pentium computer with acquisition software (Sonolab, Sonometrics, Ontario). Data were sampled at 1,600 Hz. To determine the incremental increase in pressure due to the pulse, the balloon inflation beat was subtracted from the immediately preceding control beat (Fig. 2). The transmission interval could be measured by either of two methods: 1) by shifting the base signal to best match the apex signal and by multiplying the number of sampling points shifted by the sampling interval, 0.625 ms, or 2) by

fitting the leading edge of the pressure pulses to straight lines and measuring the times of intersection with the abscissa. The first method was generally adopted during diastole, and the second method was used to increase the resolution during systolic ejection.

Having assumed that the long-axis length remained constant, we determined the zero-pressure intercept by the standard Suga-Sagawa method (13). The end-systolic pressure-area points recorded during IVC occlusion were fitted to a straight line that was extrapolated to the abscissa.

THEORY

Wave propagation in the LV is modeled by one-dimensional flow in an elastic tube. The expression for mass conservation for incompressible blood is

$$A_x + (AU)_x = 0 \quad (1)$$

where A is the cross-sectional area, U is the average velocity across the vessel, and subscript x indicates partial differentiation with respect to distance along the vessel. Neglecting viscous dissipation, the momentum equation is

$$U_t + UU_x + \frac{1}{\rho} P_x = 0 \quad (2)$$

where P is the pressure, ρ is the density of the blood, and subscript t is the partial differentiation with respect to time. Solution of these equations relies on finding a functional relationship between the vessel A and the local P (i.e., a “tube law” relationship)

$$A(x,t) = F[P(x,t); x,t] \quad (3)$$

The ventricle is considered to be an elastic conduit whose properties vary in time t . It is assumed that the properties of the wall and the flow within the ventricle can be described with a single spatial variable x , measured along the axis of the ventricle. The instantaneous ventricular pressure, $Plv(t)$,

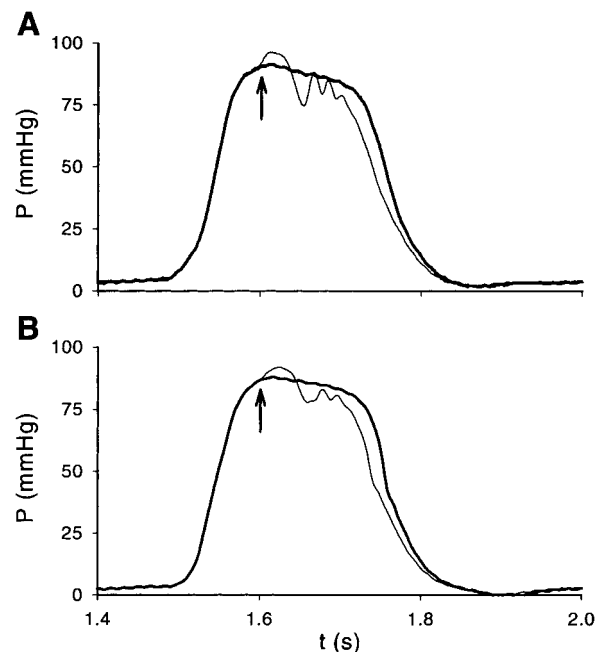


Fig. 2. The apex (A) and base (B) pressures (P) from balloon-inflation beats (thin line) superimposed on the respective control beats (thick line). Arrows signify the arrival of the pressure pulse. t , Time.

is related to the instantaneous volume of the ventricle, $V(t)$, by the elastance, $E(t)$ (8)

$$E(t) = \frac{Plv(t)}{Vlv(t) - V_d} \quad (4)$$

where $Plv(t)$ is the spatial average of the pressure $P(x,t)$, $Vlv(t)$ (where Vlv is left-ventricular volume) is the integral of $A(x,t)$ over the length of the ventricle L , and $V_d = A_d L$

$$Plv(t) = \frac{1}{L} \int_0^L P(x,t) dx$$

$$Vlv(t) = \int_0^L A(x,t) dx$$

Substituting these expressions into the definition of E , we obtain the integral relationship

$$\int_0^L \left[\frac{P}{L} - E(A - A_d) \right] dx = 0 \quad (5)$$

where A_d is the zero-pressure intercept and L is assumed to be a constant. However, variation of the long axis can easily be accommodated into the theory by setting $A(x,t) = 0$ over the part of the ventricle that is obliterated during contraction. If there is homogeneity in x (i.e., the local elastic behavior of the ventricle is the same throughout the ventricle), then the integrand must be zero

$$P(t) = LE(t)[A(t) - A_d] \quad (6)$$

This equation for the local P and A in terms of the time-varying E of the ventricle provides the tube law necessary to solve *Eqs. 1* and *2*. In the APPENDIX, these equations are written in their canonical matrix form from which the wave speed, c , can be determined by solving for the eigenvalues of the matrix in *Eq. A3*

$$c = \sqrt{\frac{ELA}{\rho}} \quad (7)$$

We note that, if we define the “compressibility” of the LV, $\gamma = ELA$, or equivalently in terms of the measurable P and A , $\gamma = PA/(A - A_d)$, then the c is simply

$$c = \sqrt{\frac{\gamma}{\rho}}$$

RESULTS

A typical result of apex-to-base transmission of the pressure pulse is shown in Fig. 3. Wave speeds varied over an order of magnitude from ~ 1 m/s during diastole to 10 m/s during systole. Figure 4 shows measured values of wave speed in temporal relation to a pressure-area loop of a representative cardiac cycle.

Figure 5 shows the log-log plots of wave speeds vs. compressibility for the six experiments in which the whole cardiac cycle was studied. The slope of the linear regression line for each dog represents the power relationship between wave speed and compressibility from the experiments ranging from 0.43 to 0.70. Pooled data are shown in Fig. 6; the regression line for the combined data yields $c = 0.974\gamma^{0.546}$, which matches well

with the theory $c = \sqrt{\gamma/\rho} = 0.976\gamma^{0.5}$, where ρ is 1,050 kg/m³ (5).

The pooled data from the negative-elastance experiments are plotted in Fig. 7 on an expanded linear scale. The regression line for the positive data is the one determined in Fig. 6. The average wave speed during periods when compressibility was negative was 1.34 m/s.

DISCUSSION

One advantage of wave-intensity analysis is that it can separate the upstream and downstream events using the pressure (dP) and velocity changes (dU) measured at a single point in the artery (6, 7, 14). With the assumption that they are additive, the dP caused by the forward and backward traveling waves can be calculated by $dP_{\pm} = \frac{1}{2}(dP \pm \rho cdU)$ and the velocity changes by $dU_{\pm} = \pm \frac{1}{2}(dP/\rho c \pm dU)$, where $+$ and $-$ signify the forward and backward waves, respectively. The power (W/m²) carried by the forward and backward waves is measured by their wave intensities, which can be calculated by $\frac{1}{4}\rho c(dP + \rho cdU)^2$ and $-\frac{1}{4}\rho c(dP - \rho cdU)^2$, respectively. Note, however, that these calculations require knowledge of the wave speed.

A wave is the result of interaction between inertial and restoring forces. When wave propagation in the LV is considered, the restoring force is due to chamber elastance, which varies continuously through the cardiac cycle. The theory shows that the square of wave speed is linearly proportional to ELA (i.e., compressibility), not elastance itself, as suggested by Shishido et al. (10). Their conclusion resulted from measurements done exclusively during isovolumic conditions when the cross-sectional area changes little. During periods in the cardiac cycle when cross-sectional area is constant, the two expressions are equivalent.

In principle, measurements of wave speed are affected by the convection of blood during systolic ejection and diastolic filling. In our experiments in which the generated pulse was propagating from the apex to the base, the measured value in systole is the wave speed plus the flow speed, and, in diastole, it is the wave speed minus the flow speed. The peak systolic flow in the outflow tract is ~ 1 m/s, which is less than one-tenth the measured systolic wave speed. In diastole, the convection due to the elastance and cross-sectional area filling waves may be more important because their peak magnitudes (~ 0.4 m/s) may be approximately one-half that of the measured wave speed. The convection correction in diastole, which increases the value of wave speed, compounded with the smaller correction in systole, which decreases the value of wave speed, tend to reduce the measured slope in the log-log plots in Figs. 5 and 6 by raising the low values and lowering the high values of wave speed. Thus correction for convection could bring the measured exponent 0.546 even closer to the theoretical value of 0.5.

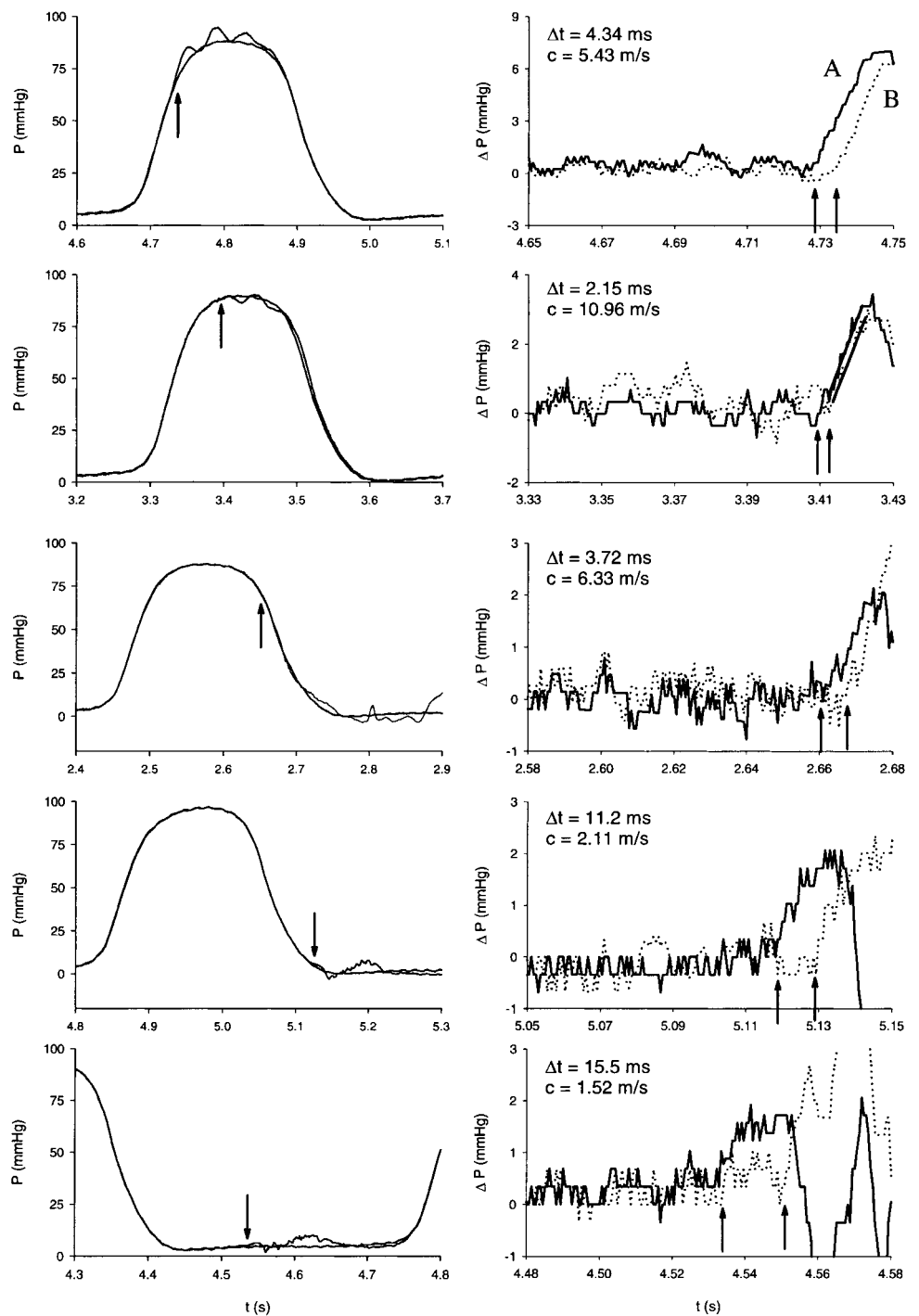


Fig. 3. Typical example (dog 6) of wave-speed measurements from early systole to end diastole. *Left*: superimposed apical LV pressures from the control and balloon inflation beats (pressures from the base not shown). The pressure of the control beat was subtracted from that of the balloon inflation beat to identify the signal due to the pressure pulse. Arrows indicate the beginning of the pulse. *Right*: these differences [change in pressure (ΔP)] from the apex (A) and base (B) are shown, plotted on the common time scale. The 2 numbers in each plot represent the transmission interval (Δt ; ms) and the calculated wave speed (c; m/s), given that the separation between the pressure transducers was 23.6 mm in this experiment. (In the second plot, the upstrokes were fitted using linear regression to improve temporal resolution.)

During diastolic filling, LV pressure sometimes falls below zero. The simple theory above predicts that negative LV pressure yields a negative elastance and an imaginary wave speed, which is not reasonable. When the transmural pressure changes from positive to negative, compression stress and bending moments may be induced with effects on wave speed that cannot be predicted from the simple theory; therefore, when elastance is negative, wave speed has to be determined experimentally. We have found that wave speeds are

consistently similar at near-zero positive and negative values of elastance.

There are limitations to this model. The shape of the LV lumen is approximately that of a hemiellipsoid, surrounded by several muscle layers arranged in different directions. The LV wall is mostly muscular, but some of the septum is membranous. Only the upper one-third of the septum is smooth and membranous, but the remainder of the inner LV wall is ridged by muscles, the trabeculae carneae. The

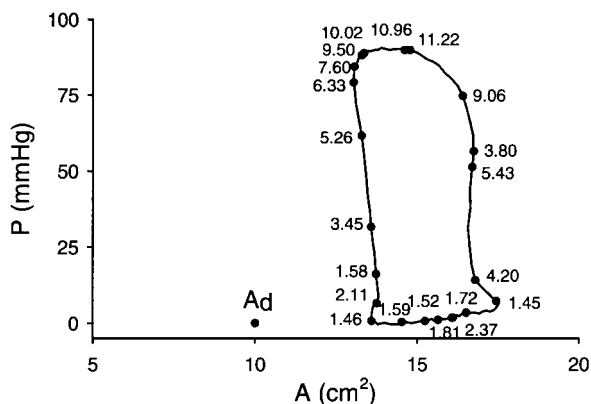


Fig. 4. To show the conceptual relation of wave speed to LV elastance (and therefore compressibility), we have plotted the wave speed measurements from *dog 6* on a representative pressure-area (A) loop. Zero-pressure intercept (A_d) for this experiment was determined to be 10 cm^2 .

wall is also thinner at the apex than the base (12). This complicated structure, however, has been simulated by using one-dimensional models with respect to the systolic ejection (15) and isovolumic contraction (10) periods. Using an *in vitro* model, Steen and Steen (11) determined that blood moves simultaneously as a flow column during early mitral filling.

The wave in the LV was assumed to travel as a plane, where the velocity is averaged across the cross-sectional area. By applying the tube law, no assumption of a uniform cross-sectional area is required, although we assumed that the long axis remained constant. We have assumed homogeneous time-varying compressibility, but this might not be true near the apex. The assumption might be improved by incorporating more complicated location-

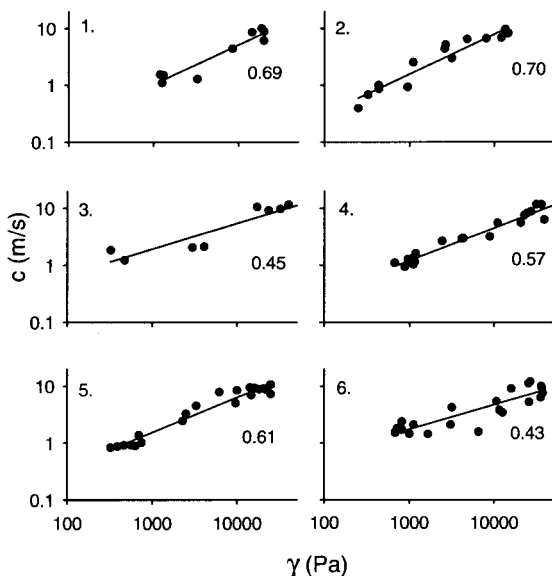


Fig. 5. Log c vs. log compressibility (γ) for the 6 experiments in which the whole cardiac cycle was studied. The slope of the best fit line determined by least squares regression for each experiment is indicated at the *right* of each regression line. The theoretical value is 0.5, and experimental values range from 0.43 to 0.70.

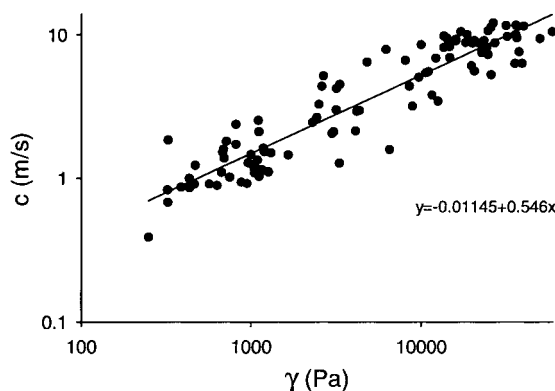


Fig. 6. Log c vs. log γ for pooled data from 6 experiments. The regression line for the pooled data yields $c = 0.974\gamma^{0.546}$.

dependent properties, which might include time-varying activation from the central left of the septum, the high anterior and apical posterior paraseptal areas (1, 2, 4).

The assumption of homogeneous time-varying compressibility implies that each part of the LV is mechanically activated simultaneously. During systole, $\sim 2 \text{ ms}$ were required for the wave to travel from one pressure transducer to the other, and, during diastole, 16 ms were required. These times are to be compared with the $\sim 12 \text{ ms}$ required for complete electrical activation (2, 3) and 22 ms for mechanical activation (4). As compressibility can be assumed to be relatively constant during diastole and as the transit time during systole was relatively small, potential effects of compressibility changing during the interval of wave transit can be ignored.

We conclude that the wave speed in the LV depends only on the instantaneous compressibility, which can be expressed in terms of the instantaneous elastance and volume of the ventricle. Our experiments showed that this relationship holds very well over the whole of the cardiac cycle during which the elastance of the ventricle varies by nearly two orders of magnitude. In the canine LV, we found $c = 0.974\gamma^{0.546} \text{ m/s}$, where $\gamma = ELA$, except when γ is negative, when the wave speed is approximately constant with $c = 1.34 \text{ m/s}$.

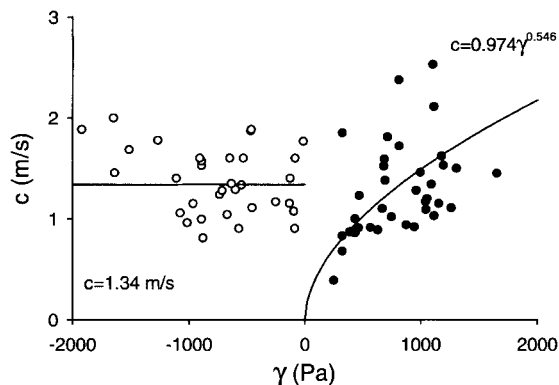


Fig. 7. Average wave speed during periods when the elastance was negative is 1.34 m/s (pooled data from 3 dogs). For γ between $-2,000$ and $2,000 \text{ Pa}$, the c is effectively constant.

APPENDIX

The relationship of cross-sectional area, local pressure, and the elastance can be stated as (Eq. 6)

$$P - EL(A - A_d) = 0$$

Differentiating, we obtain the differential relationships between the local area and the pressure and area

$$A_x = \frac{P_x}{EL}, A_t = \frac{P_t - E_t L(A - A_d)}{EL}$$

where $E_t = dE/dt$ is an ordinary differential, because of the assumption of uniform elastance. Substituting these relationships, the mass conservation equation can be written in terms of P and U

$$P_t + UP_x + ELAU_x - E_t L(A - A_d) = 0 \quad (A1)$$

The mass (Eq. A1) and momentum (Eq. 2) equations can be written in the canonical matrix form

$$\begin{pmatrix} P \\ U \end{pmatrix}_t + \begin{pmatrix} U & ELA \\ \frac{1}{\rho} & U \end{pmatrix} \begin{pmatrix} P \\ U \end{pmatrix}_x = \begin{pmatrix} E_t L(A - A_d) \\ 0 \end{pmatrix}$$

This system of equations is hyperbolic and can be solved using the method of characteristics. The eigenvalues of the matrix found from the characteristic equation

$$\begin{vmatrix} U - \lambda & ELA \\ \frac{1}{\rho} & U - \lambda \end{vmatrix} = 0$$

are $\lambda = U \pm c$, where c is defined as

$$c = \sqrt{\frac{ELA}{\rho}}$$

We acknowledge the excellent technical support provided by Cheryl Meek, Rozsa Sas, and Gerald Groves.

J. V. Tyberg is a Medical Scientist of the Alberta Heritage Foundation for Medical Research (Edmonton). The study was supported by a grant-in-aid from the Heart and Stroke Foundation of Alberta (Calgary) to J. V. Tyberg.

REFERENCES

1. **Durrer D, Roos JP, and Buller J.** The spread of excitation in canine and human hearts. In: *Electrophysiology of the Heart*, edited by Tracardi B and Marchetti G. New York: Pergamon, 1965.
2. **Durrer D, VanDam RT, Freud GE, Janse MJ, Meijler FL, and Arzbaecher RC.** Total excitation of the isolated human heart. *Circulation* 41: 899–912, 1970.
3. **Fisch C.** Electrocardiography. In: *Heart Disease: a Textbook of Cardiovascular Medicine* (5th ed.), edited by Braunwald E. Philadelphia, PA: Saunders, 1997, chapt. 4, p. 108–152.
4. **Hotta S.** The sequence of mechanical activation of the ventricle. *Jpn Circ J* 31: 1568–1572, 1967.
5. **McDonald DA.** *Blood Flow in Arteries*. London: Arnold, 1974, p. 259.
6. **Parker KH and Jones CJH.** Forward and backward running waves in the arteries: analysis using the method of characteristics. *J Biomech Eng* 112: 322–326, 1990.
7. **Parker KH, Jones CJH, Dawson JR, and Gibson DG.** What stops the flow of blood from the heart? *Heart Vessels* 4: 241–245, 1988.
8. **Sagawa K.** The ventricular pressure-volume diagram revisited. *Circ Res* 43: 677–687, 1978.
9. **Scott-Douglas NW, Traboulsi M, Smith ER, and Tyberg JV.** Experimental instrumentation and left ventricular pressure-strain relationship. *Am J Physiol Heart Circ Physiol* 261: H1693–H1697, 1991.
10. **Shishido T, Sugimachi M, Kawaguchi O, Miyano H, Kawada T, Matsuura W, Ikeda Y, and Sunagawa K.** Novel method to estimate ventricular contractility using intraventricular pulse wave velocity. *Am J Physiol Heart Circ Physiol* 277: H2409–H2415, 1999.
11. **Steen T and Steen S.** Filling of a model left ventricle studied by colour M mode Doppler. *Cardiovasc Res* 28: 1821–1827, 1994.
12. **Streeter DD.** Gross morphology and fiber geometry of the heart. In: *Handbook of Physiology. The Cardiovascular System. The Heart*. Bethesda, MD: Am. Physiol. Soc., 1979, sect. 2, vol. I, chapt. 4, p. 61–112.
13. **Suga H and Sagawa K.** Instantaneous pressure-volume relationships and their ratio in the excised, supported canine left ventricle. *Circ Res* 35: 117–126, 1974.
14. **Sun YH, Anderson TJ, Parker KH, and Tyberg JV.** Wave-intensity analysis: a new approach to coronary dynamics. *J Appl Physiol* 89: 1636–1644, 2000.
15. **Verdonck P, Vierendeels J, Riemsdagh K, and Dick E.** Left-ventricular pressure gradients: a computer-model simulation. *Med Biol Eng Comput* 37: 511–516, 1999.